PHYSICAL REVIEW B VOLUME 25, NUMBER 4 15 FEBRUARY 1982

Autocovariance functions, root-mean-square-roughness height, and autocovariance length for rough deposits of copper, silver, and gold

G. Rasigni, F. Varnier, M. Rasigni, and J. P. Palmari
Centre d'Etudes des Couches Minces, Laboratoire associé au Centre Nationale de la Recherche Scientifique, Département de Physique des Interactions Photons-Matière, Université Aix-Marseille III, Rue Henri Poincaré, 13397 Marseille Cedex 13, France

A. Llebaria
Laboratoire d'Astronomie Spatiale, 13012 Marseille, France
(Received 15 July 1981)

Autocovariance functions (ACF's) for rough surfaces of copper, silver, and gold deposits are deduced from surface profiles determined by the use of microdensitometer analysis of surface-shadowed carbon replicas. It is shown that the initial portions of the ACF's have a Gaussian form. The root-mean-square (rms) surface roughness δ and the autocorrelation length σ are deduced for each surface. Values of σ agree with corresponding values deduced from the ACF's of the surface slopes. Results of this study are compared with those previously obtained for rough magnesium deposits. We conclude that the Gaussian model is suitable to represent in general the ACF's of rough metallic surfaces. Lastly, it is shown that σ increases with δ, and within the accuracy range of their measurements there is a linear relation between δ and σ.

I. INTRODUCTION

Last year important research was undertaken about photothermal solar energy conversion. As mentioned by Seraphin and Meinel,[1] of key importance in the performance characteristics of a photothermal converter are the optical properties of the surface that intercept the solar flux and convert it into heat. These optical properties mainly depend on the surface roughness. The best way to characterize a rough surface is to determine its autocovariance function (ACF) $G(x,y)$, which summarizes statistical information on the various characteristic lengths describing the surface. Indeed, the knowledge of $G(x,y)$ as well as its Fourier transform $g(\vec{k})$ is essential to calculate the scattering and conversion to surface-plasmon oscillations of photons normally incident on the rough surface.[2]

Recently,[3,4] we developed a new method for studying surface roughness that uses a microdensitometer to analyze electron micrographs of shadowed-surface replicas. In particular, we showed that micrograph density is approximately proportional to the slopes of the surface elements, which enables us to determine the surface profile by integration of the microdensitometer data. From this hypothesis and by using different filtering algorithms, we have been able to rebuild with good accuracy the surface profile for various surfaces[4] and to compute ACF's for these surfaces.[5] We found that initial portions of ACF's had a Gaussian form for magnesium and silver deposits. It follows that $g(\vec{k})$ (the so-called surface factor) is also Gaussian. Such a result would be very important if it were true for rough metallic deposits in general. Indeed, it is interesting to know the analytical form of $g(\vec{k})$ when theoretical investigations are carried out. Moreover, for magnesium deposits of different roughness we showed that σ increases with δ and there is a linear relation between these two parameters. That conclusion disagrees with Endriz and Spicer[6] and Cunningham and Braundmeier's[7] studies. These authors find that the autocorrelation length bears an inverse relationship to the rms roughness δ. Thus the problem appears not to be completely solved and our previous conclusions require confirmation. For this purpose, we study in this paper rough deposits of copper, silver, and gold.

II. EXPERIMENTS AND CALCULATIONS

A. Preparation and characterization of deposits

The deposits of copper, silver, and gold are prepared under a static ultrahigh vacuum, i.e., in sealed ampoules in which there is a vacuum of about 10^{-9} Torr. The basic apparatus has been described previously.[8] The metal is placed in a quartz crucible and purified by high-frequency heating and successive degassing stages. Deposits are condensed on a supersmooth quartz substrate, and their structure is determined *in situ* by using a replication technique.[8] The deposits we have studied exhibited important roughness, because evaporation in sealed vessels favors surface roughness.[9] To make this roughness less important, we also prepared some deposits under dynamic vacuum (10^{-5} Torr). Some authors[7,10,11] have changed deposits roughness by depositing films of CaF_2 of different thicknesses on the quartz substrate. We did not use this procedure because it complicates the deposits preparation.

Figure 1 shows the electron photomicrographs of two surfaces of copper deposits (Cu-1 and Cu-2), silver deposits (Ag-1 and Ag-2), and gold deposits (Au-1 and Au-2). The deposits Au-2 and Cu-2 have been prepared under dynamic vacuum and all the others under static ultrahigh vacuum. All these deposits were opaque (thickness greater than 600 Å, evaporation rate roughly 10 Å/s). For most deposits, it can be seen in Fig. 1 that surface structure is characterized by a gentle undulation (rolling surface). We also attempted to prepare deposits exhibiting very important roughness. Figure 2 shows a photomicrograph of a gold deposit prepared by successive evaporations of metal without breaking vacuum.

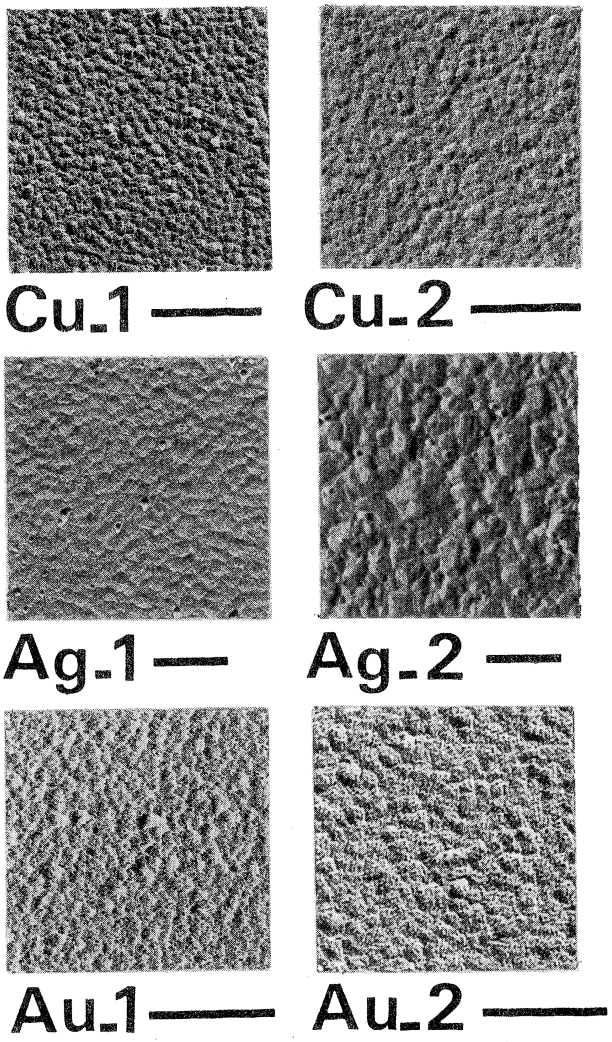

FIG. 1. Electron photomicrographs of shadowed-surface replicas for two copper deposits (Cu-1 and Cu-2), silver deposits (Ag-1 and Ag-2), and gold deposits (Au-1 and Au-2). W-Pt shadow casting at an angle of 55° for Cu-1, 65° for Cu-2, Ag-2, and Au-2, and 70° for Ag-1, Au-1. Lines represent 0.25 μm for Cu-1, Cu-2, Ag-1, Ag-2, and 0.2 μm for Au-1, Au-2.

B. Reconstruction of surface profile

The microdensitometer analysis of electron micrographs has previously been described in detail.[4] Recall that the two-dimensional analysis of the roughness structure is carried out with a processing data system microdensitometer which measures the micrograph density d at regular interval in both the x (shadow direction) and the y directions. The analysis is made line by line. Thus one obtains a grid of n scanning lines with m points per line. The principal characteristics connected with the micrograph analysis are given in Table I.

We have previously shown[4] that the slopes p of the surface elements are proportional to the micrograph density d. Thus the surface profile for a line $S(x)$ may be obtained for any x using

$$S(x)=\int_0^x p(\xi)d\xi \ . \tag{1}$$

Actually, as discussed in previous papers,[3,4] we have to eliminate random noise prior to calculations. Different filtering algorithms have therefore been used. Figure 3 shows the different steps lead-

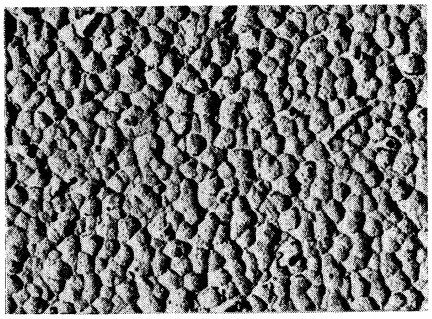

FIG. 2. Electron photomicrograph of shadowed-surface replica for a very rough deposit of gold. W-Pt shadow casting at an angle of 55°. Line represents 0.5 μm.

ing to the determination of the surface profile. The different characteristics of filtering windows are listed in Table II. It is possible to visualize the reconstruction of surface profile by plotting successive tracing of lines $S(x)$, each displaced to establish the perspective view of the surface. Figures 4 and 5 show for deposits Cu-1 and Au-3 together the photomicrograph and the perspective view of the surface obtained by means of the computer plotting program. The areas shown in the two representations are the same for Au-3 but not for Cu-1. It can be seen that a good approach of the real profile is obtained.

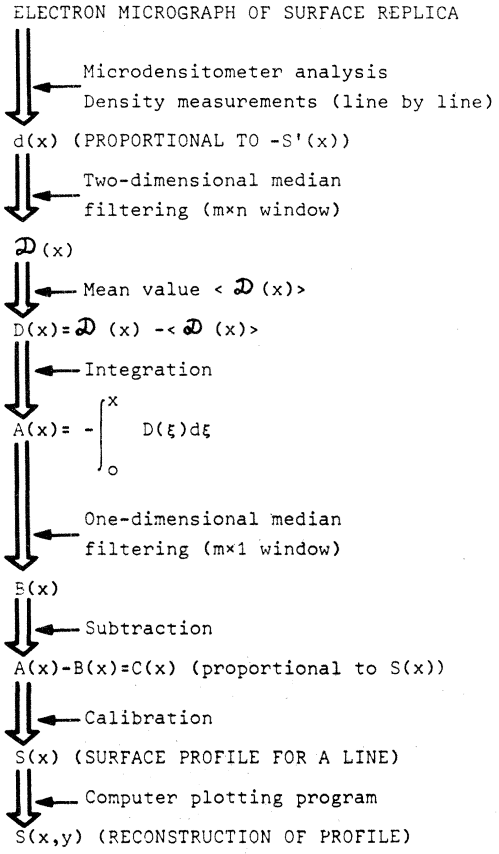

FIG. 3. Different steps of calculations leading to the determination of the surface profile.

TABLE I. Characteristics of the microdensitometer recording process. a corresponds to the microdensitometer optics, and b represents corresponding values on the real surface, taking into account micrograph magnification.

Surfaces	Micrograph magnification	Scanning spot area		x increment		y increment		Length scanned on each line	
		a (μm^2)	b (Å^2)	a (μm)	b (Å)	a (μm)	b (Å)	a (μm)	b (Å)
Copper									
Cu-1	33 000×	30×30	9.1×9.1	30	9.1	30	9.1	40 800	12 365
Cu-2	33 000×	60×60	18×18	60	18	60	18	66 000	20 000
Silver									
Ag-1	11 700×	60×60	52×52	60	52	60	52	36 960	31 690
Ag-2	15 200×	60×60	52×52	60	39.5	60	39.5	61 440	40 420
Gold									
Au-1	55 000×	40×39.8	7.3×7.2	40	7.3	40	7.3	66 000	12 000
Au-2	19 500×	30×30	15.4×15.4	30	15.4	30	15.4	55 500	28 460
Au-3	9000×	20×19.4	22×22	20	22	20	22	52 500	58 335

TABLE II. Characteristic windows for two-dimensional and one-dimensional median filtering.

Surfaces	$(m \times n)$ window two-dimensional filtering	$(m \times 1)$ window one-dimensional filtering
Copper		
Cu-1	4×4	128×1
Cu-2	4×4	80×1
Silver		
Ag-1	2×8	64×1
Ag-2	4×4	128×1
Gold		
Au-1	4×4	128×1
Au-2	4×4	90×1
Au-3	4×4	160×1

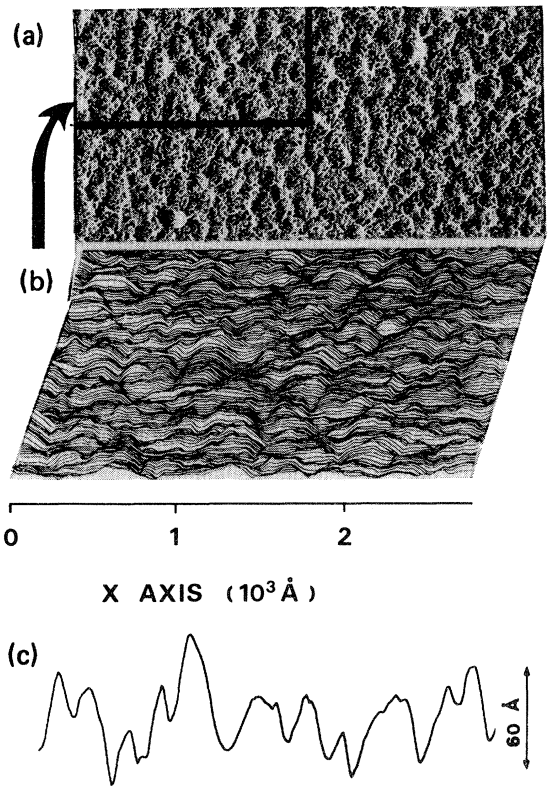

FIG. 4. (a) Electron photomicrograph of the shadowed surface carbon replica for the copper deposit Cu-1. (b) Perspective view of the surface obtained by microdensitometer analysis, using computer plotting program. The plot consists of 150 lines, 300 points by line. For convenience, only the left superior part of the photomicrograph is represented. Perspective angle 18°. (c) Represents a line of the profile.

C. Autocovariance functions

The autocovariance function for a line may be defined as[5]

$$G(x)=\lim_{a\to\infty}\frac{1}{a}\int_0^a H(x')H(x+x')dx' , \tag{2}$$

where

$$H(x)=S(x)-\langle S(x)\rangle , \tag{3}$$

and a is the distance measured on a straight line along the surface. The discrete counterparts of Eqs. (2) and (3) are computed as follows. For each line

$$\langle S\rangle=\frac{1}{N}\sum_{j=1}^{N}S_j , \tag{4}$$

where S_j is the profile connected with the jth point located on the line, and N the number of points recorded. We deduce

$$H_j=S_j-\langle S\rangle . \tag{5}$$

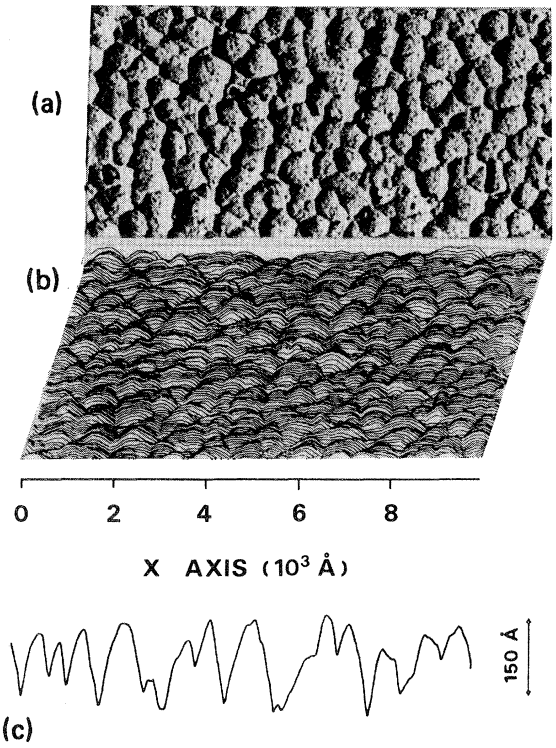

FIG. 5. Same as Fig. 4 for gold deposit Au-3. The plot consists of 225 lines, 450 points by line. For convenience every other line is represented. The areas represented in (a) and (b) are the same.

TABLE III. Characteristics of calculations for autocovariance functions $G(x)$.

Surfaces	N	$G(x)$ General trend M	p	$G(x)$ Initial portion M	p	Number of lines averaged	Number of increments between two lines
Copper							
Cu-1	1360	160	3	60	1	90	4
Cu-2	1100	160	3	60	1	63	4
Silver							
Ag-1	616	50	1	50	1	57	4
Ag-2	1024	160	2	60	1	52	4
Gold							
Au-1	1650	160	3	60	1	75	4
Au-2	1850	160	3	60	1	75	4
Au-3	2625	160	3	60	1	64	4

Values of $G(x)$ are then obtained from

$$G(m\Delta)=\frac{1}{N-M}\sum_{j=1}^{j=N-M} H_jH_{j+m} , \tag{6}$$

where Δ is the increment in the x direction, M the total number of points correlated, $m=0,1,2,\ldots,M$, and $M<<N$.

Note that in Eq. (2) the integration interval is constant. According to Elson and Bennett,[12] $G(x)$ may also be estimated in the case of a finite length a of data records by

$$G(m\Delta)=\frac{1}{N-m}\sum_{j=1}^{j=N-m} H_jH_{j+m} . \tag{7}$$

In this case, the integration interval is not constant. Actually values of $G(x)$ computed by using Eqs. (6) and (7) are in good agreement within a 5% error range.

If the distance to be correlated is large, it may be interesting, in order to reduce calculation time, to vary m by larger spaced values

$$m=0,p,2p,\ldots,M ,$$

where p is an integer larger than 1. $G(x)$ is thus computed for several regularly spaced lines, and results are given as averages over these lines. In Table III are reported the principal characteristics connected with the calculations.

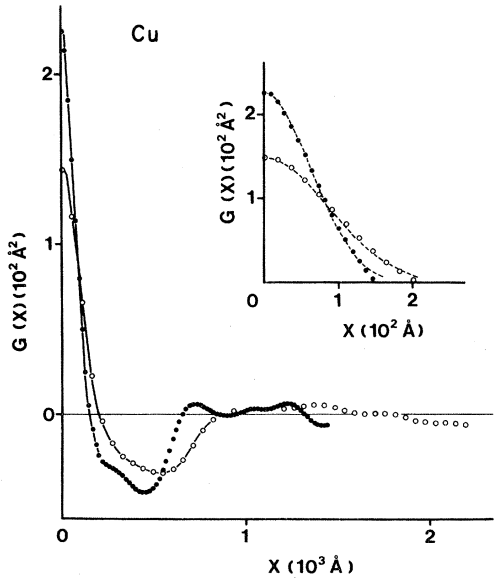

FIG. 6. Autocovariance function $G(x)$, for a surface of copper deposits Cu-1 (●—●) and Cu-2 (○—○). The initial portions of $G(x)$ are reported on an expanded x scale and the dashed curves are the Gaussian functions $G_i(x)=\delta_i^2\exp(-x^2/\sigma_i^2)$ with $\delta=15$ Å and $\sigma=87$ Å for Cu-1 and $\delta=12$ Å and $\sigma=123$ Å for Cu-2.

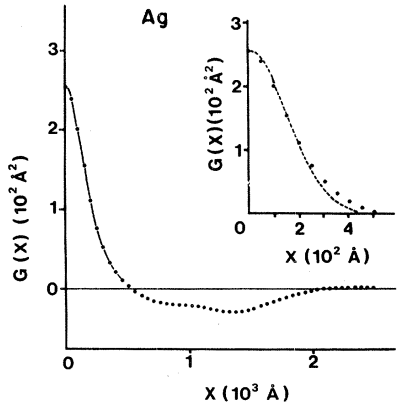

FIG. 7. Same as Fig. 6 for the silver deposit Ag-1, with $\delta=16$ Å and $\sigma=222$ Å.

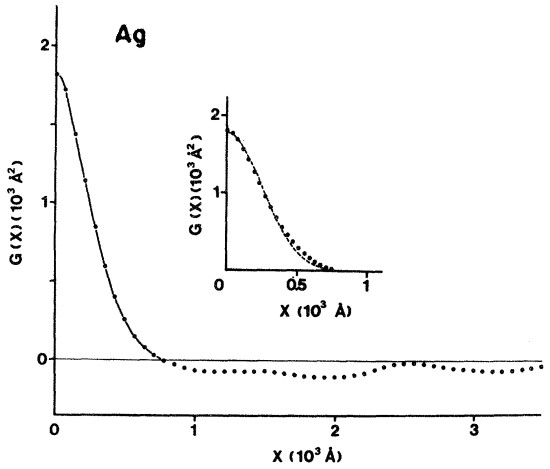

FIG. 8. Same as Fig. 6 for the silver deposit Ag-2, with $\delta=43$ Å and $\sigma=343$ Å.

III. RESULTS AND DISCUSSION

A. Shapes of ACF's

Figures 6–10 show ACF's for deposits of copper, silver, and gold, photomicrographs of which are represented in Figs. 1 and 2. The shapes of the initial portions of the ACF curves have been stated precisely by performing new calculations with values of m spaced closer together (see Table III). In Figs. 6–10, initial portions of the $G(x)$ curves are replotted in an expanded scale. The dashed curves drawn on these figures show that initial portions of $G(x)$ are fairly close to Gaussian,

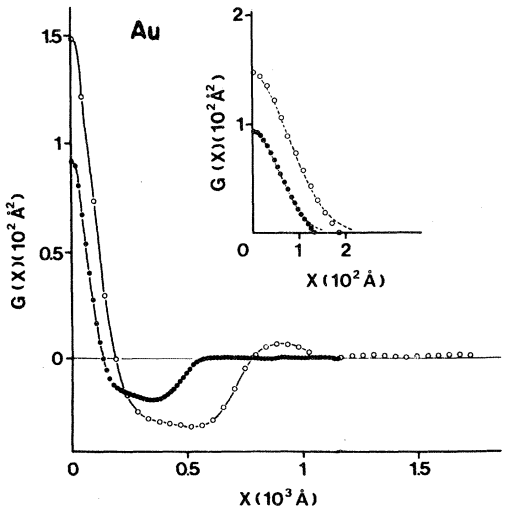

FIG. 9. Same as Fig. 6 for gold deposits Au-1 (●—●) and Au-2 (○—○) with $\delta=10$ Å and $\sigma=78$ Å for Au-1, and $\delta=12$ Å and $\sigma=110$ Å for Au-2.

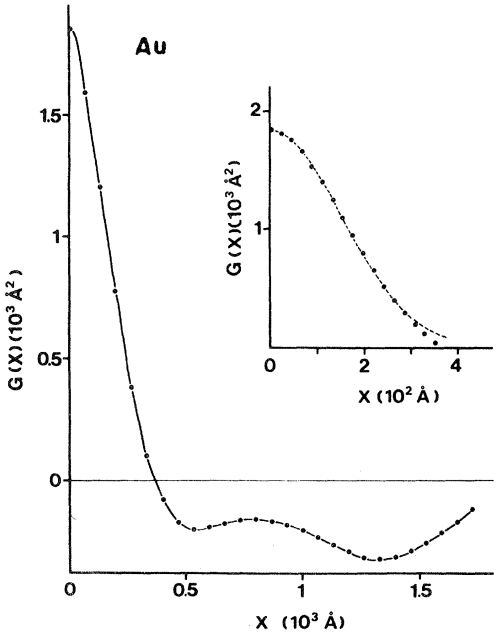

FIG. 10. Same as Fig. 6 for the gold deposit Au-3 with $\delta=43$ Å and $\sigma=217$ Å.

namely

$$G_i(x)=\delta_i^2\exp(-x^2/\sigma_i^2)\ ,\quad 0<x<(x_t)_i \tag{8}$$

where i stands for all the deposits we have studied, δ is the rms roughness height, and σ the autocorrelation length.

Let x_i^0 be the value of x corresponding to $G_i(x)=0$. This parameter has no physical significance. It is only a parameter showing (as σ_i) that the behavior of the $G_i(x)$ curves reveal with good accuracy what can be seen on microphotographs.

In Table IV are listed the values of δ_i, σ_i, $(x_t)_i$, and x_i^0 for all the deposits. These values seem suitable. For instance, the pattern structure which has lateral dimension of 220 Å on the microphotograph of deposit Cu-2 (Fig. 1) is clearly evident on the $G(x)$ tracing (Fig. 6). Similar conclusions remain for the other deposits. Let us note that the values of σ_i that are reported in Table IV lie in the range 78–343 Å and are much smaller than values heretofore reported. Indeed, the lateral resolution of our microdensitometer technique is 40 Å (see Ref. 5).

According to Eq. (8), the Fourier transform of $G(x)$ is also Gaussian, namely,

$$g_i(k)=\pi^2\delta_i^2\sigma_i^2\exp(-k^2\sigma_1^2/4)\ . \tag{9}$$

Actually, $g_i(k)$ reprsents the one-dimensional surface factor. If the surface is assumed to be isotropic (Figs. 1 and 2 show that this hypothesis is

TABLE IV. Values of different parameters characterizing the surfaces.

Surfaces	δ (Å)	σ (Å)	x_t (Å)	x^0 (Å)	$(\sigma_i)_{cal}$
Copper					
Cu-1	15	87	135	152	89
Cu-2	12	123	178	208	125
Silver					
Ag-1	16	222	256	530	212
Ag-2	43	343	355	774	314
Gold					
Au-1	10	78	113	132	81
Au-2	12	110	146	184	107
Au-3	43	217	283	368	221

quite realistic), the ACF is independent of the direction. In this case, Elson and Bennett[12] have shown that a one-dimensional ACF can be used to calculate the corresponding two-dimensional surface factor. Using the Hankel transform of $G(x)$, it may be shown[12] that $g(k)$ has also a Gaussian form.

Previously, we found after many attempts[5,13] that ACF for different roughness magnesium deposits had also a Gaussian form. These magnesium deposits were characterized by a ragged surface, different from that observed on copper, silver, and gold deposits (rolling surfaces). Thus it seems that the Gaussian model is suitable to represent in general ACF for rough metallic deposits. Moreover, for all the deposits we have studied the range of δ and σ is large enough (see Table IV) to make this conclusion general.

There is another way to verify that the values listed in Table IV are suitable. Indeed, we mentioned in Sec. II that micrograph density was proportional to the slopes of the surface roughnesses. It follows that microdensitometer data are proportional to the derivative $S'(x)$ of the profile. Let us call $G_{S'}(x)$ the ACF of the surface slopes. According to a standard relation, we have

$$G_{S'}(x) = -G''(x) , \tag{10}$$

where $G''(x)$ is the second derivative of $G(x)$ with respect to x. Given that the initial portion of $G(x)$ may be represented by a Gaussian function, we must have according to Eq. (8):

$$[G_{S'}(x)]_i = (2\delta_i^2/\sigma_i^2)(1-2x^2/\sigma_i^2) \times \exp(-x^2/\sigma_1^2) , \quad 0 < x \leq (x_t)_i .$$

In particular,

$$[G_{S'}(x)]_i = 0 ,$$

for

$$(x^0_{S'})_i = \sigma_i/\sqrt{2} . \tag{11}$$

Figures 11–14 show ACF's $G_{S'}(x)$ for all the deposits we have studied. The values of σ_i calculated according to Eq. (11), namely

$$(\sigma_i)_{cal} = \sqrt{2}(x^0_{S'})_i ,$$

are reported in Table IV. It can be seen that $(\sigma_i)_{cal}$ compare very favorably with σ_i. Note that Eq. (10) enables us to calculate $G(x)$ from $G_{S'}(x)$. We did not attempt this process because calibration of $S'(x)$ [necessary to calibrate $G_{S'}(x)$] is not easy.

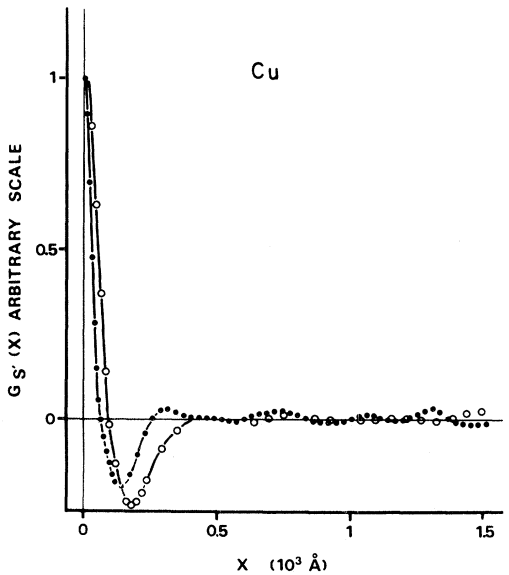

FIG. 11. Autocovariance function $G_{S'}(x)$ of the surface slopes for copper deposits Cu-1 (●—●) and Cu-2 (○—○).

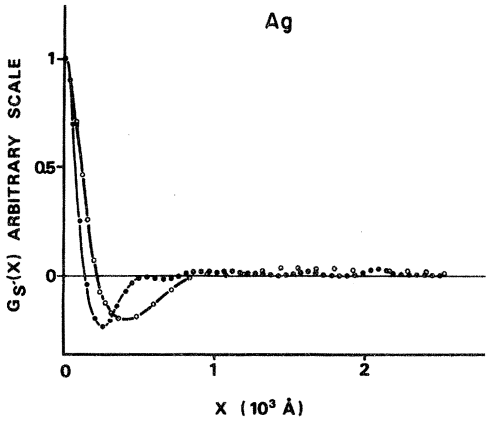

FIG. 12. Same as Fig. 11 for silver deposits Ag-1 (●—●) and Ag-2 (○—○).

B. Relationship between δ and σ

Numerous papers[5–7] have been devoted to the search for a relationship between δ and σ. This relationship might provide arguments for learning more about statisitical parameters associated with the rough surface. Recall that the dip in the optical reflectance of a solid surface at or near the surface plasma energy may be attributed to a coupling induced by the roughness.

Prior to 1970, most authors believed that for different roughness deposits σ increased with δ. This

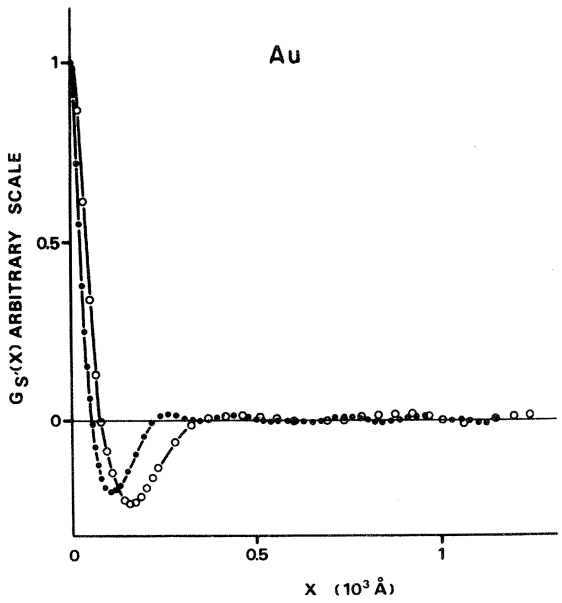

FIG. 13. Same as Fig. 11 for gold deposits Au-1 (●—●) and Au-2 (○—○).

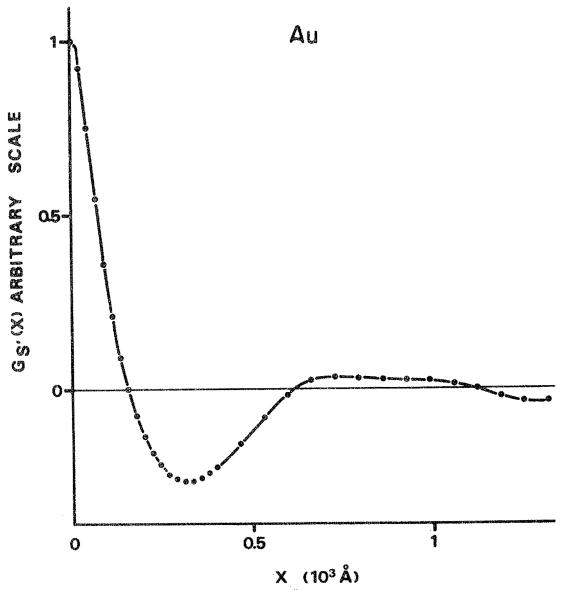

FIG. 14. Same as Fig. 11 for the gold deposit Au-3.

assumption was based on physical arguments and the observation that the reflectance minimum of a rough surface shifted to lower energy as δ increased. This argument failed when Braundmeier and Arakawa[14] showed that the surface plasmon travels with a lower phase velocity on a rough film than on a smooth film and this accounted for the shift in the reflectance minimum. In addition, Braundmeier and Hall[15] presented evidence based on surface-plasmon radiation pattern which implied that the correlation length of a surface may increase without a corresponding increase in the rms roughness. By studying aluminium rough deposits Endriz and Spicer[6] deduced that the correlation length bears an inverse relationship to the rms and Cunningham and Braundmeier[7] found that the most apparent feature of their data of σ and δ for rough silver deposits is the inverse behavior of σ and δ. These results disagree with the studies of Gesell *et al.*[16] concerning rough deposits of magnesium. By fitting their reflectance data to a theoretical expression given by Elson and Ritchie,[17] these authors deduced values of δ and σ and showed that there is a linear relation between δ and σ (σ increasing with δ). We recently confirmed this result.[5]

Figure 15 shows the variations of δ versus σ for all the deposits of copper, silver, and gold. In this figure we have also replotted the values of rough magnesium deposits we studied in a previous paper[5] and the values given by Gesell *et al.*[16] The accuracy in the determination of δ and σ is mainly

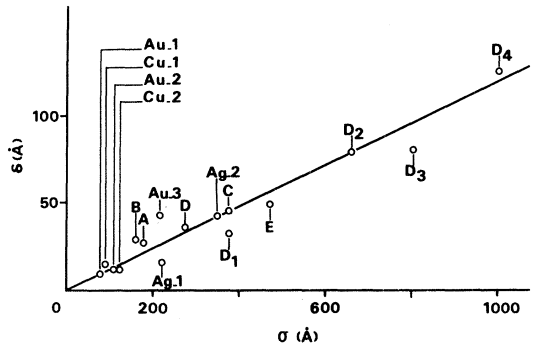

FIG. 15. Variations of the rms roughness height δ with the autocovariance length σ. D_1, D_2, D_3, and D_4 stand for the magnesium deposits studied in Ref. 13 and *A*, *B*, *C*, and *D* stand for the magnesium deposits studied by Gesell *et al.* in Ref. 16.

limited by the calibration (see discussion in Ref. 5). An accuracy of $\pm$ 10% is expected for the roughest deposits. For the smoothest deposits this estimation may be larger. Within this accuracy range, it may be considered from Fig. 15 that there is a linear relation between δ and σ (σ increasing with δ). This relation must be emphasized because it concerns the large range of δ and σ and involves different metals. Note also (Table IV) that δ is much less than a wavelength. On the other hand, σ is not much greater than a wavelength as mentioned by Eastman.[18] It ensues that δ/σ which is typical of the rms slope of the surface[19] is not indeed small compared to unity. So the scalar theory of scattering[20] cannot be used to explain properties of rough metallic deposits.

IV. CONCLUSION

Experiments that we have performed on rough deposits of copper, silver, gold, and magnesium show that the Gaussian model is suitable to represent in a general way the ACF for rough metallic surfaces. This result should stimulate theoretical considerations of the surface plasmons and diffusion problems. Concerning the relationship between δ and σ, much remains to be done. We cannot account for it at the moment. But we feel that the understanding of this relation may provide arguments for learning more about nucleation phenomenon and aid in elucidating the detailed mechanism involved in the optical process at rough interfaces.

[1]B. O. Seraphin and A. B. Meinel, in *Optical Properties of Solids,* edited by B. O. Seraphin (North-Holland, Amsterdam, 1976), p. 929.
[2]For a review of this field see H. Raether, in *Physics of Thin Films,* edited by Georg Hass (Academic, New York, 1977), Vol. 9, p. 145; R. H. Ritchie, Surf. Sci. 34, 1 (1973).
[3]M. Rasigni, G. Rasigni, J. P. Palmari, and A. Llebaria, Phys. Rev. B 23, 527 (1981).
[4]M. Rasigni, G. Rasigni, J. P. Palmari, and A. Llebaria, J. Opt. Soc. Am. 71, 1124 (1981).
[5]M. Rasigni, G. Rasigni, J. P. Palmari, and A. Llebaria J. Opt. Soc. Am. 71, 1230 (1981).
[6]J. G. Endriz and W. E. Spicer, Phys. Rev. B 4, 4144 (1971); 4, 4159 (1971).
[7]L. J. Cunningham and A. J. Braundmeier, Jr., Phys. Rev. B 14, 479 (1976).
[8]G. Rasigni, J. P. Palmari, and M. Rasigni, Phys. Rev. B 12, 1121 (1975).
[9]G. Rasigni, M. Rasigni, and J. P. Palmari, Phys. Rev. B 14, 4235 (1976).
[10]J. L. Stanford, J. Opt. Soc. Am. 60, 49 (1970).
[11]A. Daude, A. Savary, and S. Robin, J. Opt. Soc. Am. 62, 1 (1971).
[12]J. M. Elson and J. M. Bennett, J. Opt. Soc. Am. 69, 31 (1979).
[13]M. Rasigni, G. Rasigni, and J. P. Palmari, Phys. Rev. B 22, 4092 (1980).
[14]A. J. Braundmeier, Jr. and E. T. Arakawa, J. Phys. Chem. Solids 35, 517 (1974).
[15]A. J. Braundmeier, Jr. and D. G. Hall, Surf. Sci. 49, 376 (1975).
[16]T. F. Gesell, E. T. Arakawa, M. W. Williams, and R. N. Hamm, Phys. Rev. B 7, 5141 (1972).
[17]J. M. Elson and R. H. Ritchie, Phys. Rev. B 4, 4129 (1971).
[18]J. M. Eastman, in *Physics of Thin Films: Advances in Research and Development,* edited by G. Hass and M. H. Francombe (Academic, New York, 1978), Vol. 10.
[19]H. E. Bennett and J. O. Porteus, J. Opt. Soc. Am. 51, 123 (1961).
[20]P. Beckmann and A. Spizzichino, *The Scattering of Electromagnetic Waves from Rough Surfaces* (Pergamon, New York, 1963).

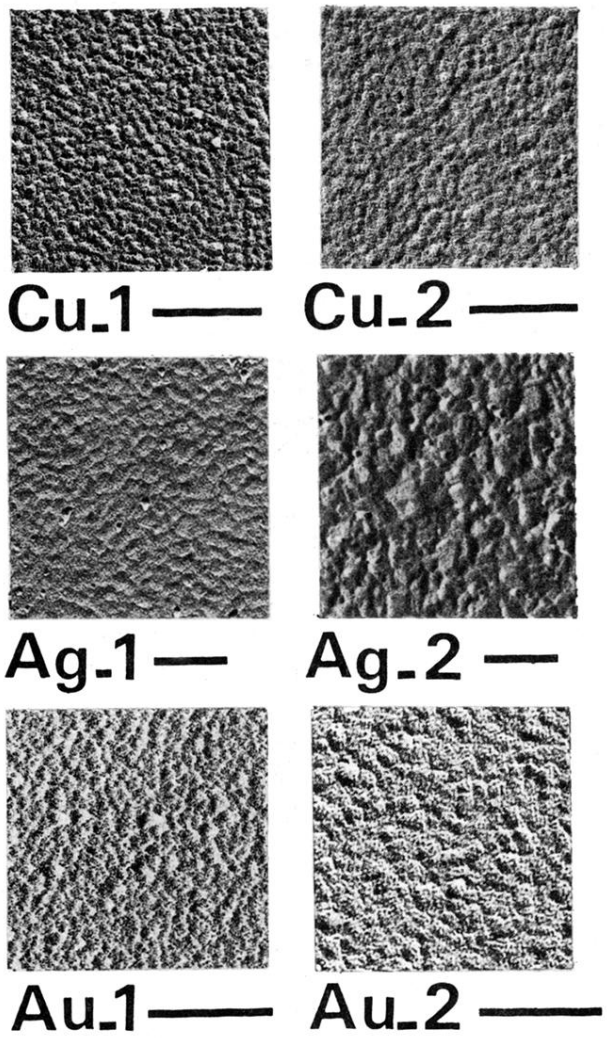

FIG. 1. Electron photomicrographs of shadowed-surface replicas for two copper deposits (Cu-1 and Cu-2), silver deposits (Ag-1 and Ag-2), and gold deposits (Au-1 and Au-2). W-Pt shadow casting at an angle of 55° for Cu-1, 65° for Cu-2, Ag-2, and Au-2, and 70° for Ag-1, Au-1. Lines represent 0.25 μm for Cu-1, Cu-2, Ag-1, Ag-2, and 0.2 μm for Au-1, Au-2.

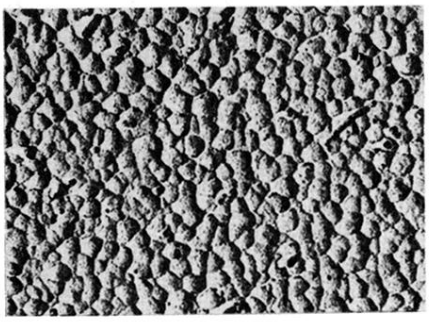

FIG. 2. Electron photomicrograph of shadowed-surface replica for a very rough deposit of gold. W-Pt shadow casting at an angle of 55°. Line represents 0.5 μm.

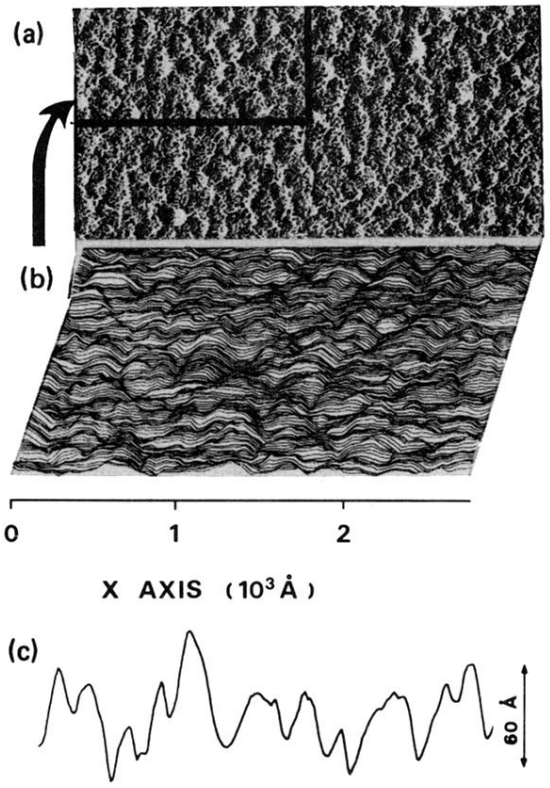

FIG. 4. (a) Electron photomicrograph of the shadowed surface carbon replica for the copper deposit Cu-1. (b) Perspective view of the surface obtained by microdensitometer analysis, using computer plotting program. The plot consists of 150 lines, 300 points by line. For convenience, only the left superior part of the photomicrograph is represented. Perspective angle 18°. (c) Represents a line of the profile.

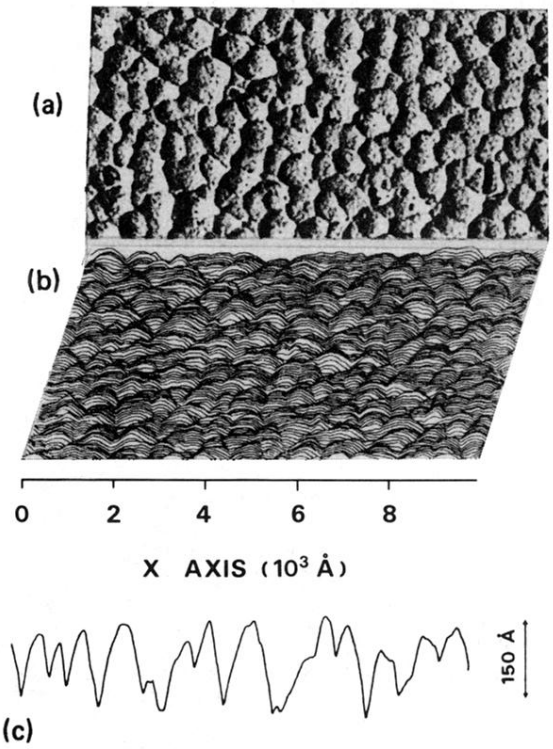

FIG. 5. Same as Fig. 4 for gold deposit Au-3. The plot consists of 225 lines, 450 points by line. For convenience every other line is represented. The areas represented in (a) and (b) are the same.